Colloid Polym Sci (2007) 285:1237–1246
DOI 10.1007/s00396-007-1676-y

ORIGINAL CONTRIBUTION

Solvent effects on the dielectric dispersion of poly(vinyl pyrrolidone)-poly(ethylene glycol) blends

R. J. Sengwa · Sonu Sankhla

Received: 6 January 2007 / Accepted: 20 March 2007 / Published online: 4 April 2007

Abstract The complex relative dielectric function $\varepsilon^*(\omega) = \varepsilon' - j\varepsilon''$, loss tangent $\tan\delta = \varepsilon''/\varepsilon'$, complex electric modulus $M^*(\omega) = M' + jM''$ and alternating current electrical conductivity dispersion behaviour of liquid poly (vinyl pyrrolidone)-poly(ethylene glycol) (PVP–PEG) blends in water, ethyl alcohol and 1,4–dioxane solvent over the entire volume mixture concentration range has been investigated in the frequency range of 20 Hz to 1 MHz at 25 °C. The PVP–PEG blends show the dielectric dispersion corresponding to the micro-Brownian motion of the PVP chain in the upper frequency region, whereas in the lower frequency region, dielectric dispersion is due to ionic conduction and electrode polarization phenomena. Results show that the conductivity values of these blends in water and dioxane can be monitored with the change in the solvent concentration, whereas it has a small variation with ethyl alcohol concentration. The comparative dielectric dispersion shape study confirms that the chain dynamics of polymers blend is influenced by heterogeneous interactions and solvent polar strength.

Keywords PVP–PEG blends · Three-phase coexisting systems · Dielectric behaviour · Chain dynamics · Conductivity relaxation

Introduction

The poly(vinyl pyrrolidone)-poly(ethylene glycol) (PVP–PEG) blends have extensive applications in pharmaceutical, cosmetic and technological industries. The solubility of PVP in low molecular weight liquid PEG is due to the formation of hydrogen bonds between the carbonyl groups of PVP monomer units and the chain ends hydroxyl groups of PEG molecules, which results in the complex structure of PVP–PEG blends. In pharmaceuticals, these blends are widely used as a transdermal drug delivery system [1, 2]. Besides the other parameters, in general, the rate of drug release in polymer matrix depends on the polymer chain dynamics and ionic conduction relaxation. Therefore, the study of polymer chain dynamics and conductivity relaxation in polymers blend, under varying conditions of composition and environment, attracts a considerable interest to explore different properties not inherent in the parent polymers.

Dielectric relaxation measurement of polymers blend provides the information about the molecular heterogeneous interactions and their dynamics [3, 4]. In the past, several attempts have been made to study the dynamics of polar solvents regarding the confirmation of their structural behaviour in PVP matrix by microwave dielectric relaxation measurements [4–11]. However, not much has been done in the frequency region of 20 Hz to 1 MHz, where the interference between ionic conduction, electrode polarization and polymer structural relaxation may be the largest, owing to the fact that in complex systems atomic, ionic or molecular units have non-trivial interactions between them [12–15]. The electrical/dielectric properties of a material are represented in terms of intensive quantities, namely, complex relative dielectric function $\varepsilon^*(\omega)$, electrical modulus $M^*(\omega)$, and electrical conductivity $\sigma^*(\omega)$ and extensive quantities, i.e. complex admittance $Y^*(\omega)$ or complex impedance $Z^*(\omega)$. In the present study, all of these presentations are used to explore various processes contributed in the electrical/dielectric properties of coexisting phases of solvent polymeric three-phase system.

R. J. Sengwa (✉) · S. Sankhla
Dielectric Research Laboratory, Department of Physics,
J N V University,
Jodhpur 342 005, India
e-mail: rjsengwa@rediffmail.com

The effect of the solvent environment on the dielectric dispersion and relaxation of polymers blend is, indeed, important because the inter-molecular interactions by the addition of a solvent can systematically be altered [4]. In this paper, dielectric study is employed to study the comparative results of the dielectric dispersion of coexisting phases of solvent polymeric three-phase systems, i.e. liquid state of PVP–PEG blends in water, ethyl alcohol (EA) and 1,4–dioxane (Dx) over the entire volume concentration range in the frequency region 20 Hz–1 MHz at 25 °C. The objective of the present paper has twofold. Firstly, to confirm the dispersion process corresponding to PVP local chain motion in PVP–PEG blend and the interactions effect of the polar solvent environment on this process. Secondly, to investigate the frequency range in which the ionic conduction and electrode surface polarization contributes to the low frequency dielectric data and their dependence on the solvent environment and concentration.

Experimental

Materials

The PVP of the average molecular weight 40,000 g mol^{-1} and the PEG of the average molecular weight 200 g mol^{-1} of the laboratory grade were obtained from Loba Chemie, India. EA and 1,4–Dx of AR grade were obtained from E. Merck, India. The PVP–PEG blends were prepared by adding 10, 20 and 30 wt% PVP in the weight of PEG. These blends were mixed in water (double distilled), EA and 1,4–Dx over six volume concentration ratios of the blend to the polar solvent, i.e. 14:86, 29:71; 43:57; 57:43; 71:29 and 86:14, respectively, for their dielectric characterisation.

Dielectric measurements

An Agilent 4284A Precision LCR meter and a four-terminal nickel-plated cobal (an alloy of 17% Cobalt+29% Nickel+54% Iron) electrode dielectric cell Agilent 16452A Liquid Test Fixture were used for the capacitance and resistance measurement in the frequency range of 20 Hz–1 MHz. The capacitance and parallel resistance of the liquid dielectric test fixture, without and with samples, were measured to compensate for a short. The test fixture correction coefficient was also considered to cancel the effect of stray capacitance during the evaluation of the values of complex relative dielectric function. All measurements were made at 25 °C, and the temperature was controlled by the Thermo-Haake DC10 controller with a precision of ±0.01 °C.

The complex relative dielectric function ε*(ω) is determined from the relation [16]

$$\varepsilon^*(\omega) = \varepsilon' - j\varepsilon'' = \alpha\left(\frac{C_P}{C_o} - j\frac{1}{\omega C_o R_P}\right), \tag{1}$$

where $\omega = 2\pi f$ is the angular frequency, C_o and C_P are the capacitances of the free space and with sample, respectively; R_P is the equivalent parallel resistance of the cell with the sample, and α is the correction coefficient of the cell.

Data analysis and results

Figures 1, 2 and 3 show the spectra of the real part of the relative dielectric function ε′, the dielectric loss ε″ and loss tangent $\tan\delta = \varepsilon''/\varepsilon'$ of the PVP–PEG blend with 30 wt% PVP concentration and its volume mixtures in water, EA and Dx at 25 °C.

The broadband values of $\varepsilon^*(\omega) = \varepsilon' - j\varepsilon''$ for the solutions of polymer blends, in the 20 Hz–20 GHz frequency range, can be well described by a sum of the three relaxation processes with the contribution of direct current (dc) conductivity σ_o by the equation [5]:

$$\varepsilon^*(\omega) = \varepsilon_\infty + \Delta\varepsilon_l^*(\omega) + \Delta\varepsilon_m^*(\omega) + \Delta\varepsilon_h^*(\omega) - j(\sigma_o/\omega\varepsilon_o), \tag{2}$$

where ε_o is the dielectric permittivity in vacuum, ε_∞ is the high-frequency limiting dielectric permittivity, Δε is the dielectric relaxation strength and the subscripts *l*, *m* and *h* denote the low-, middle- and high-frequency processes, respectively.

The low-frequency process for polymer blends is caused by the electrode polarization. When an electric field is applied to the materials, then the long-range drift of ions and barrier layer formation on the electrode surface result in large values of the relative dielectric function [12–15, 17, 18].

The dielectric loss ε″ spectra peak of the *l*-process of the PVP–PEG blend is outside the lower-frequency limit of our experimental frequency range (it is below 20 Hz), only its high-frequency tail is observed (Figs. 1, 2 and 3). The observed *m*-process in the upper frequency range of the present study corresponds to the micro-Brownian motion (local chain motion) of the PVP chain, which is highlighted in the insets of Figs. 1, 2 and 3. The *h*-process corresponds to the re-orientation motion of small-sized polar molecules, which occurs in the microwave frequency region. We are concerned only in the *l*- and *m*-processes in the present study of the complex systems.

The real part σ' and the imaginary part σ'' of the alternating current (ac) complex conductivity, $\sigma^*(\omega)$ of the polymers blend, were obtained from the relation

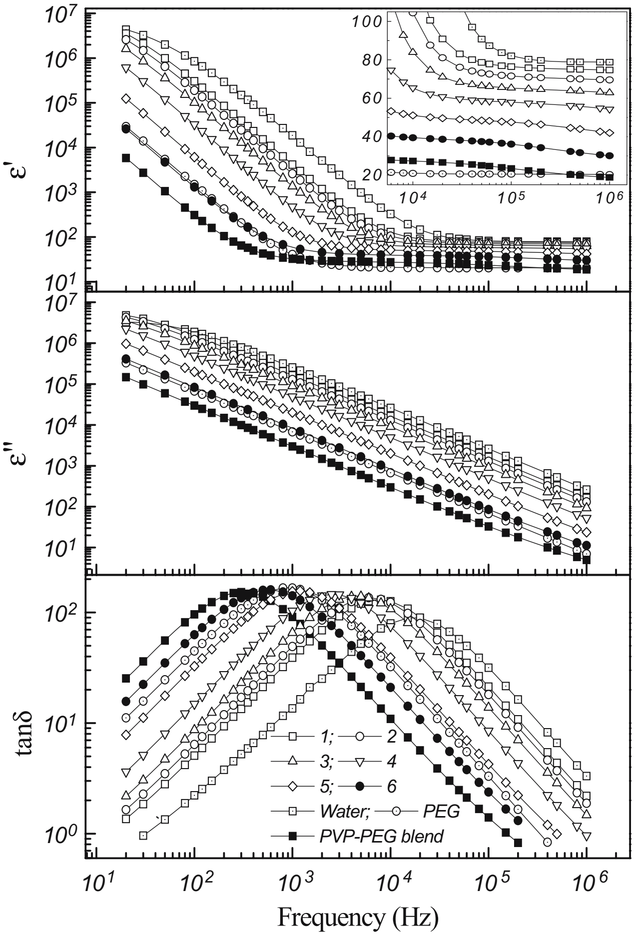

Fig. 1 Frequency dependence of the real part of the relative dielectric function ε′, dielectric loss ε″ and loss tangent *tanδ* of water (W), poly (ethylene glycol) (PEG200) and poly(vinyl pyrrolidone)-poly(ethylene glycol) (*PVP–PEG*) blend with 30 wt% PVP and that of the PVP–PEG blend in water at volume percentage ratios [PVP–PEG blend:W] (1) 14:86, (2) 29:71, (3) 43:57, (4) 57:43, (5) 71:29 and (6) 86:14. Inset shows that the gradual shift of the *m*-process corresponds to the local chain motion of PVP towards higher frequencies with the increase in water concentration in the blend. For clarity, *error bars* are not indicated. *Error bars* are smaller than the size of the symbols

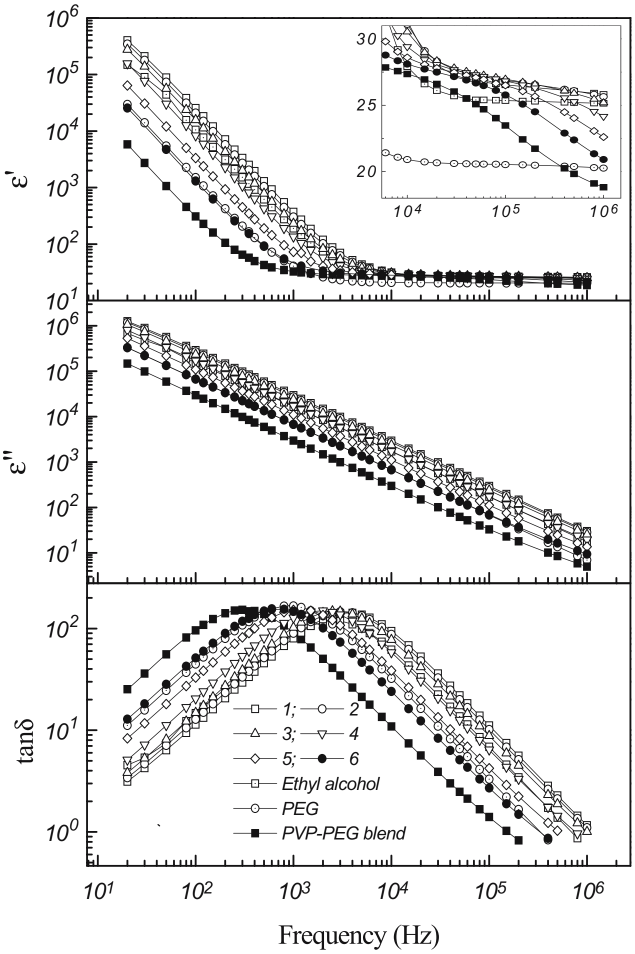

Fig. 2 Frequency dependence of the real part of the relative dielectric function ε′, dielectric loss ε″ and loss tangent *tanδ* of ethyl alcohol (EA), poly(ethylene glycol) (PEG200) and poly(vinyl pyrrolidone)-poly (ethylene glycol) (*PVP–PEG*) blend with 30 wt% PVP and that of the PVP–PEG blend in ethyl alcohol at volume percentage ratios [PVP–PEG blend:EA] (1) 14:86, (2) 29:71, (3) 43:57, (4) 57:43, (5) 71:29 and (6) 86:14. Inset shows that the gradual shift of the *m*-process corresponds to the local chain motion of PVP towards higher frequencies with the increase in ethyl alcohol concentration in the blend. For clarity, *error bars* are not indicated. *Error bars* are smaller than the size of the symbols

$$\sigma^*(\omega) = \sigma' + j\sigma'' = j\omega\varepsilon_o\varepsilon^*(\omega) = \omega\varepsilon_o\varepsilon'' + j\omega\varepsilon_o\varepsilon'. \tag{3}$$

Figures 4, 5 and 6 show the variation of the σ' values of the solutions of PVP–PEG blends against frequency in water, EA and Dx. At low frequencies, $\sigma'(\omega)$ is a constant at the dc value σ_o. For a fixed temperature, σ' increases at high frequencies according to a power law $\sigma' \sim \omega^s$, where $0<s\leq 1$. It is usual to express $\sigma'(\omega)$ as the empirical relation [19]

$$\sigma'(\omega) = \sigma'_{\mathrm{dc}} + A\omega^S \tag{4}$$

where A is a constant dependent on temperature T and $\sigma'_{\mathrm{dc}} = \sigma_o$. The s values of the PVP–PEG blends were observed in the range ≈ 0.77 to 1.0.

Considering the charges as the independent variable, conductivity relaxation effects can be suitably analysed within the modulus formalism in terms of a dimensionless quantity, $M^*(\omega)$. Analogous to mechanical relaxation, the electric modulus M^* is obtained from the relation [17, 18, 20]

$$\begin{aligned} M^*(\omega) &= \frac{1}{\varepsilon^*(\omega)} = M' + jM'' \\ &= \frac{\varepsilon'}{\varepsilon'^2 + \varepsilon''^2} + j\frac{\varepsilon''}{\varepsilon'^2 + \varepsilon''^2}. \end{aligned} \tag{5}$$

The main advantage of this formulation is that the space charge effects often do not mask the features of the spectra, owing to the suppression of high capacitance phenomena in $M''(f)$ plots. The variation of the evaluated

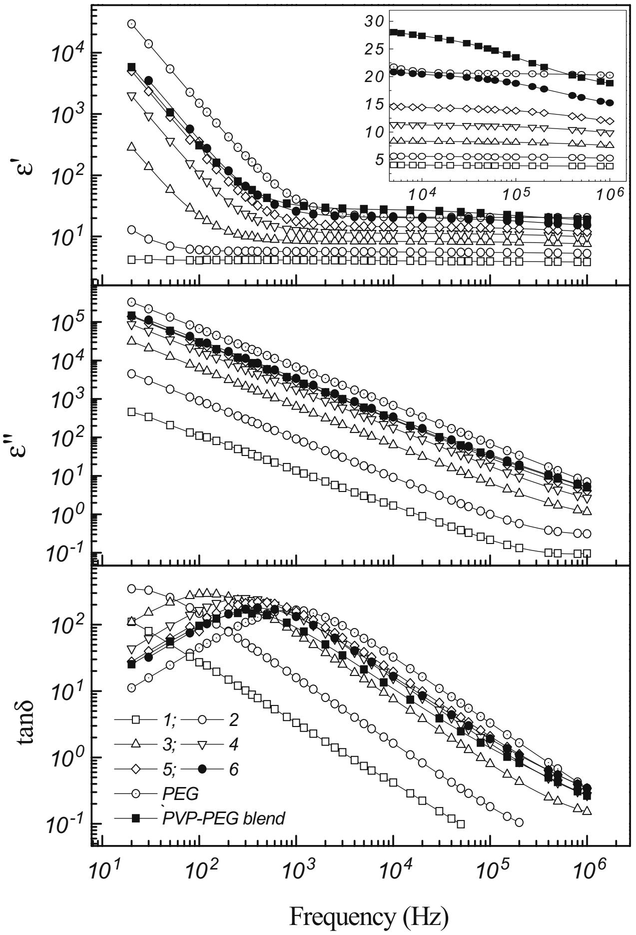

Fig. 3 Frequency dependence of the real part of the relative dielectric function ε′, dielectric loss ε″ and loss tangent *tanδ* of poly(ethylene glycol) (PEG200) and poly(vinyl pyrrolidone)-poly(ethylene glycol) (*PVP–PEG*) blend with 30 wt% PVP and that of the PVP–PEG blend in dioxane (Dx) at volume percentage ratios [PVP–PEG blend:Dx] (1) 14:86, (2) 29:71, (3) 43:57, (4) 57:43, (5) 71:29 and (6) 86:14. Inset shows that the gradual shift of the *m*-process corresponds to the local chain motion of PVP towards higher frequencies with the increase in dioxane concentration in the blend. For clarity, *error bars* are not indicated. *Error bars* are smaller than the size of the symbols

values of M' and M'' vs f of the PVP–PEG blend along with its different volume ratio mixture in water, EA and Dx are shown in Figs. 4, 5 and 6. The $M''(f)$ spectra of these materials have a peak, and the frequency (f_σ) corresponding to it is related to the ionic conductivity relaxation (the change from dc to ac transport), where both charge carrier transport and polymer local chain motion may contribute to the electric field relaxation. Finally, the electrical modulus can be written as [21]:

$$M^*(\omega) = M_\infty \frac{j\omega\tau_\sigma}{1+j\omega\tau_\sigma} = \frac{1}{\varepsilon_\infty}\left[\frac{(\omega\tau_\sigma)^2}{1+(\omega\tau_\sigma)^2} + j\frac{(\omega\tau_\sigma)}{1+(\omega\tau_\sigma)^2}\right] \tag{6}$$

where τ_σ is the most probable ionic conductivity relaxation time, and ε_∞ is the relaxed (high frequency) dielectric permittivity of the matrix. In Eq. 6 of the electrical modulus conductivity relaxation, at $\omega_\sigma = 2\pi f_\sigma = 1/\tau_\sigma$ it is $M'=M''$, where M'' also has a local maximum. Therefore, the τ_σ values were obtained directly from the value of frequency f_σ corresponding to the peak of M'' spectrum [21]. The M'' data were fit using the Origin® non-linear curve fitting tool to find the correct value of f_σ. In the case of water solvent, the f_σ values were determined up to ~0.4 volume fraction of water in the PVP–PEG blend. For higher water concentration, the fit data did not show the peak in M'' because it shifted much above the upper frequency limit of our experimental range, i.e. 1 MHz.

To investigate the most probable ionic conductivity relaxation time τ_σ and electrode polarization relaxation time τ_{EP}, the frequency-dependent master curves of real and imaginary parts of ε*, M^* and σ^* and tanδ for the PVP–PEG blend with 30 wt% PVP concentration are plotted in Fig. 7. In Fig. 7, the strong upturn of ε′ at low frequency

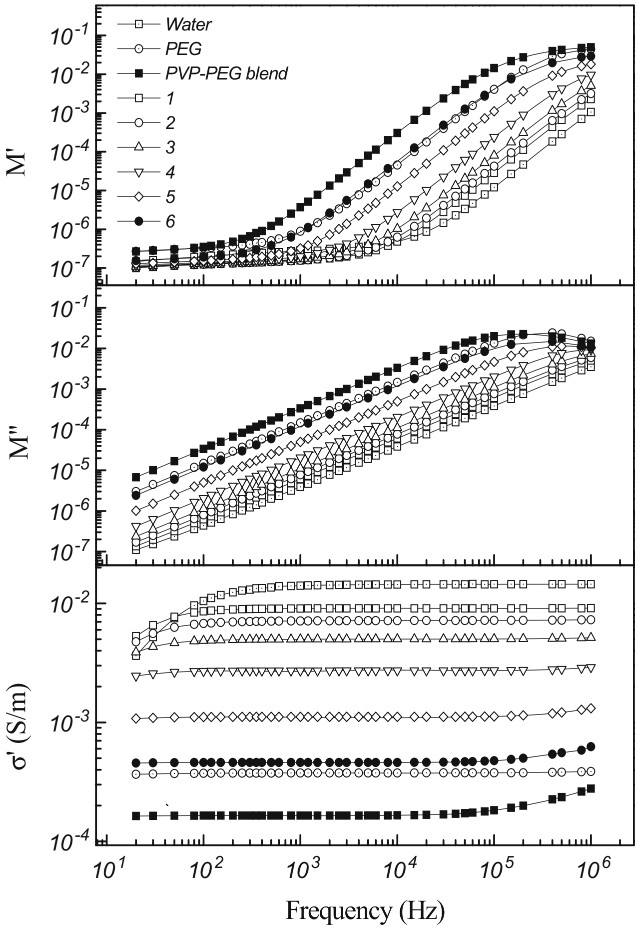

Fig. 4 Frequency dependence of the real part of the electric modulus M', modulus loss M'' and the real part of the ac conductivity σ' of water (W), poly(ethylene glycol) (PEG200) and poly(vinyl pyrrolidone)-poly(ethylene glycol) (*PVP–PEG*) blend in water at volume percentage ratios [PVP–PEG blend:W] (1) 14:86, (2) 29:71, (3) 43:57, (4) 57:43, (5) 71:29 and (6) 86:14. For clarity, *error bars* are not indicated. *Error bars* are smaller than the size of the symbols

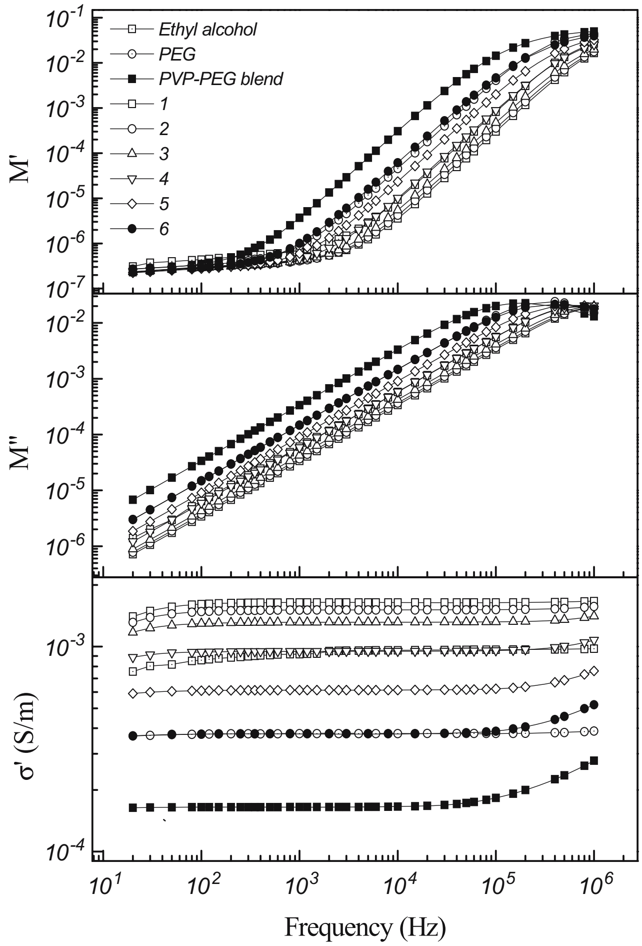

Fig. 5 Frequency dependence of the real part of the electric modulus *M*′, modulus loss *M*″ and real part of the ac conductivity σ' of ethyl alcohol (EA), poly(ethylene glycol) (PEG200) and poly(vinyl pyrrolidone)-poly(ethylene glycol) (*PVP–PEG*) blend in ethyl alcohol at volume percentage ratios [PVP–PEG blend:EA] (1) 14:86, (2) 29:71, (3) 43:57, (4) 57:43, (5) 71:29 and (6) 86:14. For clarity, *error bars* are not indicated. *Error bars* are smaller than the size of the symbols

arises from the accumulation of ions at the electrode interface, i.e. the so-called electrode polarization (EP) effect. From the master curves, it is observed that the tanδ peak frequency f_{EP} is closely related to the strong upturn frequency of ε′, and the electrode polarization relaxation time τ_{EP} was determined from the relation $\tau_{\mathrm{EP}} = 1/2\pi f_{\mathrm{EP}}$, which involves the charging/discharging of double layer capacitance [15]. In the case of the PVP–PEG blend with 30 wt% PVP, the f_{EP} is ~300 Hz.

The complex impedance formalism $Z^*(\omega)$ is commonly used to separate the bulk and the surface phenomena [12–14, 20]. A common feature of dielectrics with dc conductivity is a discontinuity at the electrode/dielectric interface, which has different polarization properties than the bulk of the dielectric. The complex impedance of the polymers blends were evaluated by the relation

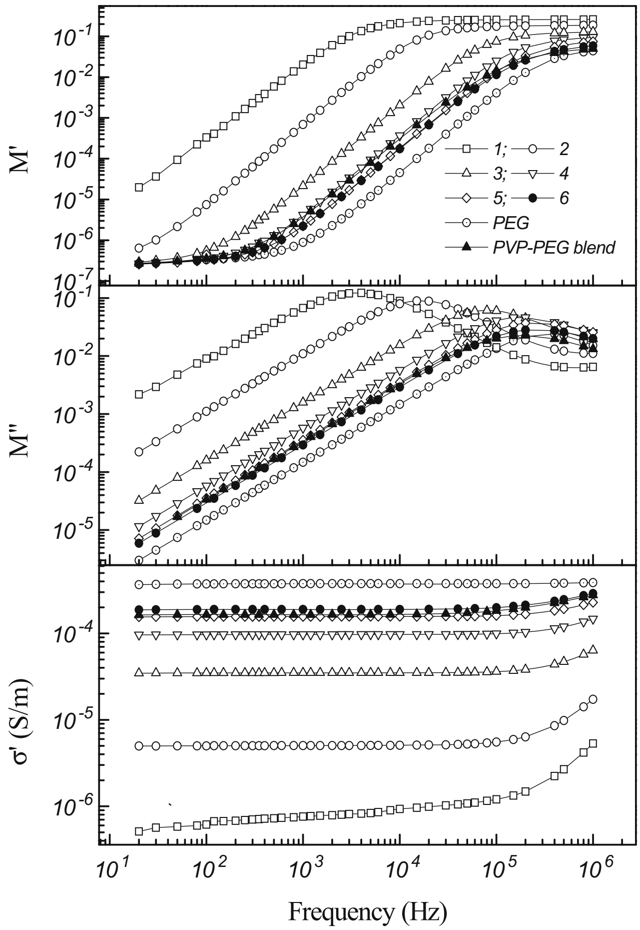

Fig. 6 Frequency dependence of the real part of the electric modulus *M*′, modulus loss *M*″ and real part of the ac conductivity σ' of poly (ethylene glycol) (PEG200) and poly(vinyl pyrrolidone)-poly(ethylene glycol) (*PVP–PEG*) blend in dioxane at volume percentage ratios [PVP–PEG blend:Dx] (1) 14:86, (2) 29:71, (3) 43:57, (4) 57:43, (5) 71:29 and (6) 86:14. For clarity, *error bars* are not indicated. *Error bars* are smaller than the size of the symbols

$$\begin{aligned} Z^*(\omega) &= \frac{1}{Y^*(\omega)} = Z' - jZ'' \\ &= \frac{R_P}{1 + (\omega C_P R_P)^2} - j\frac{\omega C_P R_P^2}{1 + (\omega C_P R_P)^2}. \end{aligned} \tag{7}$$

The complex impedance plane plot (Z'' vs Z') is plotted in Fig. 8 for the PVP–PEG blend to confirm the electrode polarization frequency f_{EP}, which separates the bulk and electrode polarization phenomena. The inset of Fig. 8 shows that the f_{EP} value, which separates the bulk and electrode surface phenomena, is exactly equal to the tanδ peak frequency. Therefore, we use the tan$\delta(f)$ plots to evaluate the τ_{EP} values of the PVP–PEG blend in different solvents. The exact value of f_{EP} is determined by fitting the data to the Origin® non-linear curve fitting tool. The evaluated values of the τ_σ, τ_{EP} and σ_{o} for the PVP–PEG blend in solutions of water, EA and Dx are plotted against

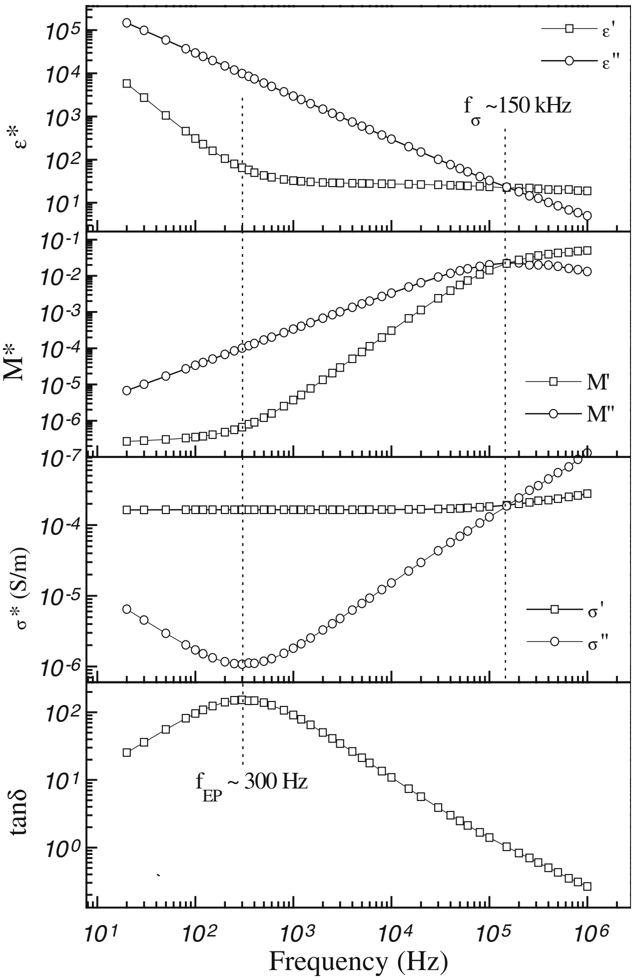

Fig. 7 Simultaneous superpositions of the real and imaginary parts of the complex relative dielectric function ε*, the electric modulus *M**, the complex conductivity *σ** and the loss tangent *tanδ* for poly(vinyl pyrrolidone)-poly(ethylene glycol) (*PVP–PEG*) blend with 30 wt% PVP concentration at 25 °C. The superposition is observed at the *M*″ maximum frequency. For clarity, *error bars* are not indicated. *Error*

the volume fraction of the solvent in Fig. 9. These values were fitted to a fourth order polynomial equation

$$Y = \mathrm{A} + \mathrm{B1}X^1 + \mathrm{B2}X^2 + \mathrm{B3}X^3 + \mathrm{B4}X^4 \tag{8}$$

using the Origin® non-linear curve fitting tool. The values for the coefficients of Eq. 8, i.e. A, B1, B2, B3 and B4 are listed in Table 1 along with the standard deviation, SD, of the fit for the PVP–PEG blend in different solvents.

Discussion

Complex dielectric behaviour

Figures 1, 2 and 3 show that the PVP–PEG blend with 30 wt% PVP concentration has the dielectric dispersion in the upper frequency region of our experimental frequency range, which is corresponding to the micro-Brownian motion (local chain segmental motion) of the PVP chain (*m*-process) [5]. The *m*-process dispersion suggests that the complex structure of PVP–PEG blend is in dynamic equilibrium, which is due to the breaking and reforming of heterogeneous hydrogen bonds between the carbonyl groups of PVP monomer units and the chain ends hydroxyl groups of PEG molecules. Identical to this, the dielectric dispersion curves of the *m*-process were also found for the PVP–PEG blends of 10 and 20 wt% PVP concentration (not shown in this paper). However, the dielectric dispersion range, i.e. dielectric strength of the *m*-process, increases as the concentration of PVP increases in the PVP–PEG blends.

The comparative shapes of the *m*-process dielectric dispersion (insets of Figs. 1, 2 and 3) of the PVP–PEG blend in water, EA and Dx solvent have the gradual shift towards higher frequencies with the increase of solvent concentration and it shifts above 1 MHz for the solvent-rich solutions of the blends. Further, insets of figures also confirm that there is no dielectric dispersion corresponding to the chain segmental motion (*m*-process) of the PEG molecules, and it has only molecular re-orientational dynamics in the microwave frequency region [22]. When the PVP–PEG blend is added into the solvent, the small-sized molecules of the solvent penetrate into the heterogeneous complex structure of the blend because of which the PVP–PEG structure gets elongated [9, 23]. As the solvent concentration increases, the PVP–PEG structure gets more elongated and hence, hindrance is reduced to the PVP chain segmental motion, and correspondingly, there is a gradual shift of their *m*-process dielectric dispersion towards more higher frequency region [9, 10,

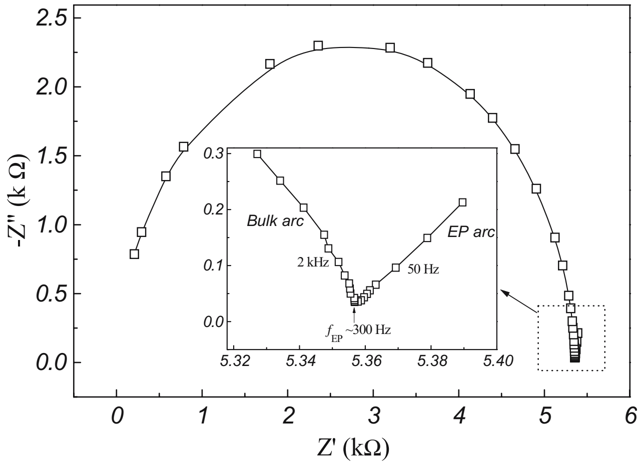

Fig. 8 Complex impedance plane plot (*Z*″ vs *Z*′) for poly(vinyl pyrrolidone)-poly(ethylene glycol) (*PVP–PEG*) blend with 30 wt% PVP concentration at 25 °C. Inset shows the frequency of *Z*″ minimum, which separates the bulk and electrode polarization phenomena. For clarity, *error bars* are not indicated. *Error bars* are smaller than the size of the symbols

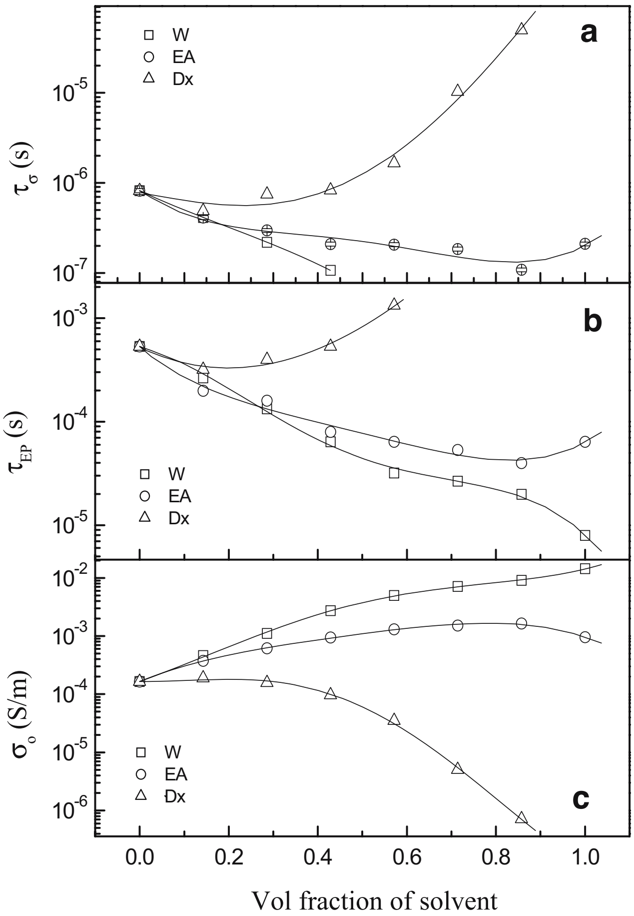

Fig. 9 Solvent concentration dependence of the most probable ionic conductivity relaxation time τ_σ, the electrode polarization relaxation time τ_{EP}, and the dc conductivity σ_o of the poly(vinyl pyrrolidone)-poly(ethylene glycol) (*PVP–PEG*) blend in water (*W*), ethyl alcohol (*EA*) and dioxane (*Dx*) solvent at 25 °C. The *lines* are non-linear fits with the fit parameters indicated in Table 1. For clarity, *error bars* are indicated only on one plot of **a**. These *error bars* are according to the size of the symbols

23, 24]. Although the molecules of water, EA and Dx form complexes with the PVP and PEG molecules [6–8, 10, 11, 25] through hydrogen bonds, the shape of the dispersion curves suggests that the PVP–PEG blend structure elongation masks the hindrance effect produced by the formation of solvent complexes with the blend structure in regards to the micro-Brownian motion of the PVP chain. The decrease in the viscosity with the increase in solvent concentration in the PVP–PEG blend cannot be ruled out in the shift of the *m*-process in the higher frequency region for solvent-rich solutions of the PVP–PEG blend.

The PVP–PEG blends and their solutions in water, EA and Dx have a large increase in the values of complex dielectric constant with the decrease in frequency in the lower frequency region (Figs. 1, 2 and 3), which is mainly due to ionic conduction and electrode polarization [5, 12–15]. Further, the low frequency ε′ values monotonously increases with the increase in water concentration, which may be due to the high static permittivity of water molecules and their large contribution in electrode polarization effect; whereas the ε′ values in Dx solvent of the low static permittivity decreases monotonously with the increase in Dx concentration in the PVP–PEG blends. It seems that because of nearly equal values of static permittivity of PEG and EA molecules, the PVP–PEG blends in EA solvent have anomalous variation in ε′ values with the change in EA concentration. Recently [25], authors have investigated the heterogeneous interaction behaviour of PEG–water, PEG–EA and PEG–Dx over the entire concentration range by a static dielectric permittivity measurement and by determination of the Kirkwood correlation factor, which confirms the entirely different heterogeneous interaction behaviour of water, EA and Dx with PEG molecules. The different interaction behaviour of PEG with these solvent molecules is also reflected in

Table 1 Coefficients A, B1, B2, B3 and B4 of the nonlinear equation with its standard deviation (SD) for the values of ionic conduction relaxation time (τ_σ), electrode polarization relaxation time (τ_{EP}) and dc conductivity σ_o of the PVP–PEG blend in different solvents at 25 °C shown in Fig. 9

System	A	B1	B2	B3	B4	SD
Non-linear fit parameters of τ_σ values						
PVP–PEG blend in water	−6.087	−2.314	2.069	−3.461	–	0.000
PVP–PEG blend in ethyl alcohol	−6.074	−3.689	11.313	−16.705	8.453	0.087
PVP–PEG blend in dioxane	−6.108	−0.885	−0.592	8.522	−4.350	0.138
Non-linear fit parameters of τ_{EP} values						
PVP–PEG blend in water	−3.286	−0.833	−8.651	16.518	−8.839	0.047
PVP–PEG blend in ethyl alcohol	−3.282	−3.580	7.960	−11.182	5.882	0.071
PVP–PEG blend in dioxane	−3.282	−2.061	5.588	−1.331	–	0.064
Non-linear fit parameters of σ_o values						
PVP–PEG blend in water	−3.776	2.592	3.445	−8.804	4.697	0.022
PVP–PEG blend in ethyl alcohol	−3.782	3.182	−5.917	7.880	−4.376	0.020
PVP–PEG blend in dioxane	−3.775	−0.236	5.072	−17.468	9.447	0.054

the ε′ spectra of the PVP–PEG blend over the frequency range of 20 Hz–1 MHz. The comparative study of the *m*-process dispersion of the PVP–PEG blends confirm that the PVP chain segmental dielectric relaxation is very sensitive to the solvent environment.

The ε″ values of the PVP–PEG blends in water, EA and Dx solvent decrease with the increase in frequency (Figs. 1, 2 and 3). In the case of pure blend and also at low concentration of the solvent, these spectra indicate the dielectric loss dispersion corresponding to the *m*-process in the upper frequency region. Figures 1, 2 and 3 also include a variation of the values of loss tangent ($\tan\delta = \varepsilon''/\varepsilon'$) of these complex systems against frequency. It is found that all the solutions of the blends have a tan*δ* peak magnitude of about 100. The large tan*δ* peak value of the PVP-polar solvent blends may be due to the presence of some common ionic impurity traces in the polar solvents. Further, the tan*δ*(*f*) peak shows the gradual shift towards higher frequencies as the concentration of water and EA increases in the solutions of the PVP–PEG blends, whereas reverse behaviour is found in the Dx solvent. The observed tan*δ* peak frequency values are corresponding to the frequency that separates the bulk and surface phenomena (dielectric/electrode interface) contributed in the values of low frequency complex relative dielectric function [15].

From tan*δ* plots, the upper frequency limit of the electrode polarization effect for water is found to be ~20 kHz, which decreases with the increase of PVP–PEG blend concentration in water solutions, and for pure PVP–PEG blend, it is ~300 Hz. These findings confirm that the thickness of electrode surface barrier layers arises because of the adsorption of the PVP–PEG blends on the electrode surfaces, which increases in presence of a water solvent [26]. Similar behaviour is also found in the case of the PVP–PEG blends in EA solutions. However, for EA, the upper frequency range value of the electrode polarization is ~3 kHz, which is much lower than the corresponding frequency limit value of water. In the case of the PVP–PEG blend in Dx solution, the electrode polarization frequency range has a gradual decrease from 300 Hz with an increase in Dx concentration in PVP–PEG blend, and in the Dx-rich solutions of the blend, this range is lower than 20 Hz. The decrease in the electrode polarization frequency range of the PVP–PEG blends in Dx solutions is expected because of its weak polar behaviour, which resists the formation of the PVP–PEG blend layers on the surfaces of nickel-plated cobal electrodes of the dielectric cell.

Electric modulus behaviour

Figures 4 and 5 show that the PVP–PEG blend solutions in water and EA solvent have the peak in *M*″(*f*) spectra for higher concentrations of the blend in the frequency range of 10^5–10^6 Hz. Further, frequency corresponding to the *M*″ peak value has gradually shifted towards higher frequencies with the increase in these solvent concentrations in the blend. However, in the case of the PVP–PEG blend solutions in the Dx solvent, the frequency corresponding to the *M*″ peak value has shifted towards the lower frequency region as the concentration of Dx increases in the solutions (Fig. 6). These observations indicate that the shift in *M*″ peak on the frequency scale of PVP–PEG blends have comparative opposite behaviour in the solutions of strong polar solvents as compared to weak or non-polar solvents. The *M*″ peak frequency (f_σ) of the solutions of the PVP–PEG blends is related to the ionic conductivity relaxation time ($\tau_\sigma = 1/2\pi f_\sigma$), i.e. the change from dc to ac transport, in which both charge carrier transport and polymer local chain motion contribute to the electric field relaxation, which is discussed in detail in the section of 'master curve representation' [12, 15, 27].

AC conductivity behaviour

The real part of the ac conductivity σ' of the PVP–PEG blends in water solutions increases with the increase in water concentration (Fig. 4), which is because of the higher conductivity value of water. Further, PVP–PEG blend in water solution shows the conductivity relaxation at a higher concentration of the blend, which indicates the change from dc to ac transport in the frequency range of 10^4–10^6 Hz, where the peak in *M*″(*f*) spectra were also observed. Figure 4 shows that all the PVP–PEG blends in water solutions have the plateaus of σ' in the lower frequency region, i.e. frequency independent values of conductivity, which corresponds to dc conductivity σ_o. Although all the solutions of the PVP–PEG blends in EA have the plateaus of σ' in the lower frequency region, the values vary anomalously with small magnitude for the increase in EA concentration (Fig. 5). The PVP–PEG blend-rich solutions in EA have a slight lower conductivity, whereas the EA-rich PVP–PEG solutions have slight higher conductivity as compared to the conductivity of pure EA. The conductivity values of PVP–PEG blends in EA confirms that there is a negligible variation in the overall conductive structure of the PVP–PEG blend in the EA solutions. This may be due to the polymeric chain type self-associated structure of EA molecules [6–8] and its heterogeneous interactions with the super molecular structure of the PVP–PEG blend [28], which form an identical conductive structure to the PVP–PEG blend itself [6–8].

The σ' value of the PVP–PEG blends in Dx solutions decreases with the increase of the Dx concentration (Fig. 6), which is expected because of the weak polar behaviour of the Dx. Further, these solutions have the plateaus of σ' in the lower frequency region and also show the conductivity relaxation in the upper frequency region. The conductivity spectra of the PVP–PEG blend in water and Dx solvent clearly indicates that their conductivity values can be monitored by changing the solvent concentration in the solutions of the PVP–PEG blends. Further, it is observed that the frequency values corresponding to the tanδ peak and the M'' peak have approximately three order scale differences in all the blend solutions despite the large difference in the polar behaviour of the solvents.

At the upper frequency region, the real part of the ac conductivity σ' of the PVP–PEG blend and the blend-rich solutions in polar solvents follows a power law $\sigma'(\omega) \propto \omega^s$. The PVP–PEG blend with 30 wt% PVP concentration has the s value of 0.77, whereas the solutions of the blend in water and EA shows the s values ≈ 0.8–0.98. In the case of the solutions of the blend in the Dx solvent, s values are close to unity.

Master curves representation

It can be clearly seen from the master curves (Fig. 7) that the intersection of the real and imaginary parts of all intensive quantities of PVP–PEG blend occurs at the same frequency, below which dc conduction dominates. The superpositions were observed exactly at the M'' maximum frequency. Similar results were also found for solutions at higher blend concentration of PVP–PEG blends in water, EA and Dx solvent. Recently Runt et al. [15, 21, 29, 30] extensively investigated the ionic conduction and electrode polarization and their modeling in polymer electrolytes using dielectric relaxation spectroscopy over the frequency range of 0.01 Hz–10 MHz and applied the master curves representation to evaluate the values of τ_σ and τ_{EP}. It was found that the τ_σ values decreases for PVP–PEG blends in water and EA solvent with the increase in solvent concentration, which confirms the increase in the local segmental mobility of the PVP chain; whereas in the case of the Dx solvent, τ_σ increases with the increase in Dx concentration in the PVP–PEG blend. From these observations, it can be concluded that the segmental motion of the PVP–PEG blend is facilitated by a strong H–bond forming solvent because of the dynamic equilibrium of the H-bonded structure as compared to the weakly and non-polar solvent.

As can be clearly seen from Fig. 9a, b, the trend of the variation of τ_{EP} is identical to the τ_σ with the increase of the solvent concentration, but conductivity relaxation is much faster than the electrode polarization relaxation.

Figure 9c shows the dc ionic conductivity σ_o variation with the solvent concentration of the PVP–PEG blend. It was found that the σ_o value of the PVP–PEG blend increases in water and EA solvent, whereas it decreases significantly in the Dx solvent at a higher concentration.

Conclusions

This paper presents the measured electrical/dielectric data in terms of (1) complex relative dielectric function, (2) loss tangent, (3) electric modulus, (4) ac conductivity and (5) complex impedance of the PVP–PEG blend and its solutions in weak and strong polar solvents in the frequency range of 20 Hz–1 MHz for the confirmation of electrode polarization relaxation, ionic conduction relaxation and segmental motion behaviour. These blends have lower frequency range dielectric dispersion, which is governed by ionic conduction and electrode polarization. The upper frequency range dielectric dispersion is corresponding to the PVP chain segmental motion in the dynamic equilibrium of the PVP–PEG complex structure, which is significantly influenced by the polar strength of the solvent. The conductivity values of the solutions of the PVP–PEG blends in the strong polar solvent (water) and in the weak polar solvent (Dx) can be monitored by changing the solvent concentration, whereas the PVP–PEG blends in the EA solvent show small change in conductivity value with concentration, which is because of the linear polymeric structure of EA molecules. From this study, interesting results on ionic conduction relaxation and electrode polarization relaxation have been obtained for the PVP–PEG blend in coexisting phases of solvent polymeric three phase system at only 25 °C, which may be a starting point for further studies on these complex systems by varying temperature over a wide frequency range.

Acknowledgement The work was done as a part of the project no. SR/S2/CMP-9/2002 financed by the Department of Science and Technology, New Delhi, India.

References

1. Feldstein MM, Tohmakhchi VN, Malkhzov LB, Vasiliev AE, Plate NA (1996) Int J Pharm 131:229–242
2. Feldstein MM, Raigorodskii IM, Iordanski AL, Hadgraft JJ (1998) Control Release 52:25–40
3. Kremer F, Schonhals A (2002) Broadband dielectric spectroscopy. Springer, Berlin Heidelberg New York
4. Havriliak S Jr, Havriliak SJ (1997) Dielectric and mechanical relaxation in materials: interpretation and applications to polymers. Verlag, Munich
5. Shinyashiki N, Sengwa RJ, Tsubotani S, Nakamura H, Sudo S, Yagihara S (2006) J Phys Chem A 110:4953–4957
6. Sengwa RJ, Abhilasha, More NM (2003) Polymer 44:2577–2583
7. Sengwa RJ, Abhilasha, More NM, Mehrotra SC (2005) J Polym Sci B Polym Phys 43:1134–1143
8. Sengwa RJ, Abhilasha, Mehrotra SC, Sharma BR (2004) Indian J Phys 78:1341–1348
9. Sengwa RJ (2003) Polym Int 52:1462–1467
10. Sengwa RJ, Sankhla S, Abhilasha (2005) Indian J Phys 79:879–886
11. Sengwa RJ, Sankhla S (2006) Pramana–J Phys 67:375–381
12. Pissis P, Kyritsis A (1997) Solid State Ionics 97:105–113

13. Kyritsis A, Pissis P (1997) J Polym Sci Polym Phys 35:1545–1560
14. Macdonald JR (1987) Impedance spectroscopy—emphasizing solid materials and systems. Wiley, New York
15. Klein RJ, Zhang S, Dou S, Jones BH, Colby RH, Runt J (2006) J Chem Phys 124:144903–144910
16. Agilent Technologies (2000) Agilent 16452A liquid test fixture—operation and service manual. Agilent, Japan
17. Macedo PB, Moynihan CT, Bose R (1972) Phys Chem Glasses 13:171–179
18. Hasz WC, Moynihan CT, Tick PA (1994) J Non-Cryst Solids 172–174:1363–1368
19. Moynihan CT (1994) J Non-Cryst Solids 172–174:1395–1403
20. Kyritsis A, Pissis P, Grammatikakis J (1995) J Polym Sci B Polym Phys 33:1737–1750
21. Zhang S, Dou S, Colby RH, Runt J (2005) J Non-Cryst Solids 351:2825–2830
22. Sengwa RJ, Kaur K, Chaudhary R (2000) Polym Int 49:599–608
23. Fried JR (1995) Polymer science and technology. Prentice-Hall, Englewood Cliffs
24. Sengwa RJ, Abhilasha (2004) Indian J Pure Appl Phys 42:142–148
25. Sengwa RJ, Sankhla S (2007) J Mol Liq 130:119–131
26. Craig DQM, Newton JM, Hill RM (1993) J Mater Sci 28:405–410
27. Monedero MA, Luengo GS, Moreno S, Ortega F, Rubio RG, Prolongo MG, Masegosa RM (1999) Polymer 40:5833–5842
28. Feldstein MM, Lebedeva TL, Shandryuk GA, Kotomin SV, Kuptsov SA, Igonin VE, Grokhovskaya TE, Kulichikhin VG (1999) Polymer Sci Ser A 41:854–866
29. Zhang S, Runt J (2004) J Phys Chem B 108:6295–6302
30. Dou S, Zhang S, Klein RJ, Runt J, Colby RH (2006) Chem Mater 18:4288–4295